The EMBO Journal (2006) 25, 3357–3366 | © 2006 European Molecular Biology Organization | All Rights Reserved 0261-4189/06
www.embojournal.org

THE EMBO JOURNAL

HDAC6–p97/VCP controlled polyubiquitin chain turnover

Cyril Boyault[1], Benoit Gilquin[1], Yu Zhang[2], Vladimir Rybin[3], Elspeth Garman[4], Wolfram Meyer-Klaucke[5], Patrick Matthias[2], Christoph W Müller[6,*] and Saadi Khochbin[1,*]

[1]INSERM U309, Laboratoire de Biologie Moléculaire et Cellulaire de la Différenciation, Equipe chromatine et expression des gènes, Institut Albert Bonniot, Faculté de Médecine, Domaine de la Merci, La Tronche, France, [2]Friedrich Miescher Institute for Biomedical Research, Novartis Research Foundation, Basel, Switzerland, [3]European Molecular Biology Laboratory, Heidelberg, Germany, [4]Laboratory of Molecular Biophysics, Department of Biochemistry, Oxford University, Oxford, UK, [5]European Molecular Biology Laboratory, Hamburg, Germany and [6]European Molecular Biology Laboratory, Grenoble, France

HDAC6 is a unique cytoplasmic deacetylase capable of interacting with ubiquitin. Using a combination of biophysical, biochemical and biological approaches, we have characterized the ubiquitin-binding domain of HDAC6, named ZnF-UBP, and investigated its biological functions. These studies show that the three Zn ion-containing HDAC6 ZnF-UBP domain presents the highest known affinity for ubiquitin monomers and mediates the ability of HDAC6 to negatively control the cellular polyubiquitin chain turnover. We further show that HDAC6-interacting chaperone, p97/VCP, dissociates the HDAC6–ubiquitin complexes and counteracts the ability of HDAC6 to promote the accumulation of polyubiquitinated proteins. We propose that a finely tuned balance of HDAC6 and p97/VCP concentrations determines the fate of ubiquitinated misfolded proteins: p97/VCP would promote protein degradation and ubiquitin turnover, whereas HDAC6 would favour the accumulation of ubiquitinated protein aggregates and inclusion body formation.

The EMBO Journal (2006) **25,** 3357–3366. doi:10.1038/sj.emboj.7601210; Published online 29 June 2006
Subject Categories: proteins; molecular biology of disease
Keywords: CFTR; E4; neurodegenerative diseases; USP; zinc-finger

*Corresponding authors. S Khochbin, Laboratoire de Biologie Moléculaire et Cellulaire, de la Différenciation, INSERM U309, Equipe chromatine et expression des gènes, Institut Albert Bonniot, Faculté de Médecine, Domaine de la Merci, 38706 La Tronche, France.
Tel.: +33 4 76 54 95 83; Fax: +33 4 76 54 95 95;
E-mail: khochbin@ujf-grenoble.fr or CW Müller, European Molecular Biology Laboratory, Grenoble Outstation, BP 181, 38042 Grenoble Cedex 9, France. Tel.: +33 476 20 75 61; Fax: +33 476 20 71 99;
E-mail: mueller@embl-grenoble.fr

Received: 8 December 2005; accepted: 31 May 2006; published online: 29 June 2006

Introduction

HDAC6, a member of class II HDACs, was first identified in the mouse (Verdel *et al*, 1999), and both the mouse and its human orthologue were shown to deacetylate histones *in vitro* (Grozinger *et al*, 1999; Verdel *et al*, 1999). Its first identified physiological substrate was however the cytoplasmic protein α-tubulin (Hubbert *et al*, 2002; Matsuyama *et al*, 2002; Zhang *et al*, 2003). In agreement with this finding, the early functional studies of mouse HDAC6 showed that it is actively maintained in the cytoplasm (Verdel *et al*, 2000). Moreover, its human orthologue contains an additional domain responsible for a stable maintenance of HDAC6 in the cytoplasm (Bertos *et al*, 2004), suggesting that the protein functions primarily in this compartment. HDAC6 contains a region of homology with the non-catalytic domain of several ubiquitin-specific proteases (USPs) known as ZnF-UBP (Amerik *et al*, 2000). HDAC6 ZnF-UBP domain interacts efficiently with free or bound monomeric ubiquitin (Seigneurin-Berny *et al*, 2001), as well as with polyubiquitin chains (Hook *et al*, 2002). The purification of an HDAC6-containing complex from mouse testis cytosolic extracts showed that HDAC6 is associated with at least two proteins homologous to yeast proteins involved in the ubiquitin fusion and degradation (UFD) pathway (Seigneurin-Berny *et al*, 2001). One of these proteins is the phospholipase A2 activating protein, a mouse orthologue of the yeast UFD3 involved in cellular ubiquitin turnover (Johnson *et al*, 1995). The other is the well-known AAA-ATPase chaperone, p97/VCP, which also interacts with UFD3 (Ghislain *et al*, 1996; Mullally *et al*, 2006; Rumpf and Jentsch, 2006).

HDAC6 deacetylase activity may control the stability of the dynamic pool of microtubules through an unknown mechanism (Matsuyama *et al*, 2002). It may also coordinate microtubules and actin networks (Destaing *et al*, 2005) and finally, by deacetylating its second known substrate, HSP90, it may also control the chaperone activity of this protein (Kovacs *et al*, 2005).

Less is known about the function of HDAC6 ubiquitin-binding activity. HDAC6, through its simultaneous binding to minus end-directed dynein motors and to ubiquitinated protein aggregates, is thought to act as an adaptor, linking these aggregates to the moving microtubules in order to achieve the formation of the so-called cellular aggresomes (Kawaguchi *et al*, 2003).

Here, using a series of biophysical approaches, we first characterized the ZnF-UBP domain of HDAC6. These experiments showed that HDAC6 ZnF-UBP binds one ubiquitin molecule with the highest known affinity. The combination of particle-induced X-ray emission (PIXE) and extended X-ray absorption fine structure (EXAFS) revealed the presence of three zinc atoms per molecule of HDAC6 ZnF-UBP ligated on average by one histidine and three cysteine residues. Biochemical and biological studies, including the use of cell lines from HDAC6$^{-/-}$ mice re-expressing wild type or a non-

ubiquitin-binding HDAC6 mutant, showed that the high-affinity binding of ubiquitin by HDAC6 stabilizes poly-ubiquitin chains and favours the formation of aggresomes containing cystic fibrosis transmembrane conducting regulator (CFTR). Interestingly, the HDAC6 partner, p97/VCP, dissociates HDAC6–ubiquitin complexes and hence regulates the ubiquitin-dependent functions of HDAC6. This work shows for the first time that a finely tuned balance of HDAC6 and p97/VCP concentrations defines the stability of the pool of ubiquitinated proteins and determines their fate.

Results

HDAC6 ZnF-UBP binds ubiquitin with high affinity

In order to better characterize HDAC6 ZnF-UBP domain, we first selected a portion of the HDAC6 C-terminal region spanning residues 1000–1149, which includes the entire USP homology region (Figure 1A, see also Figure 2B). The corresponding encoding sequence was cloned in an expression vector and the protein expressed and purified (data not shown).

Gel filtration (Pharmacia Superdex 75) analysis showed that the ZnF-UBP domain eluted at a volume of 11.9 ml compatible with the ZnF-UBP domain being an elongated monomer or forming dimers. ZnF-UBP and ubiquitin co-eluted at 11.4 ml, suggesting that both components associate at an equimolar ratio (Figure 1B). Sedimentation equilibrium experiments of ubiquitin, HDAC6 ZnF-UBP domain and HDAC6 ZnF-UBP domain/ubiquitin complex yielded masses of 11.3, 17.5 and 28.3 kDa, respectively, which is in excellent agreement with their molecular weights (His-ubiquitin: 11.5 kDa; HDAC6 ZnF-UBP domain: 17.0 kDa; HDAC6 ZnF-UBP domain/ubiquitin complex: 28.5 kDa) (Figure 1C). Similar results were obtained in sedimentation velocity experiments (data not shown). Our results demonstrate that the ZnF-UBP domain and ubiquitin are monomeric in solution and that they associate in a 1:1 complex.

The binding of ubiquitin to the HDAC6 ZnF-UBP domain was studied quantitatively using isothermal titration calorimetry (ITC; Figure 1D). The affinity of the HDAC6 ZnF-UBP domain to ubiquitin is high with a calculated equilibrium constant (K_D) of 60 nM and a stoichiometry of 1:1 ($N = 1.071 + 0.004$). The ΔH for the binding of ubiquitin to the HDAC6 ZnF-UBP domain is $\Delta H = -17.9 + 0.1$ kcal/mol, suggesting a substantial number of non-covalent interactions between both partners. In comparison, the USP5 ZnF-UBP

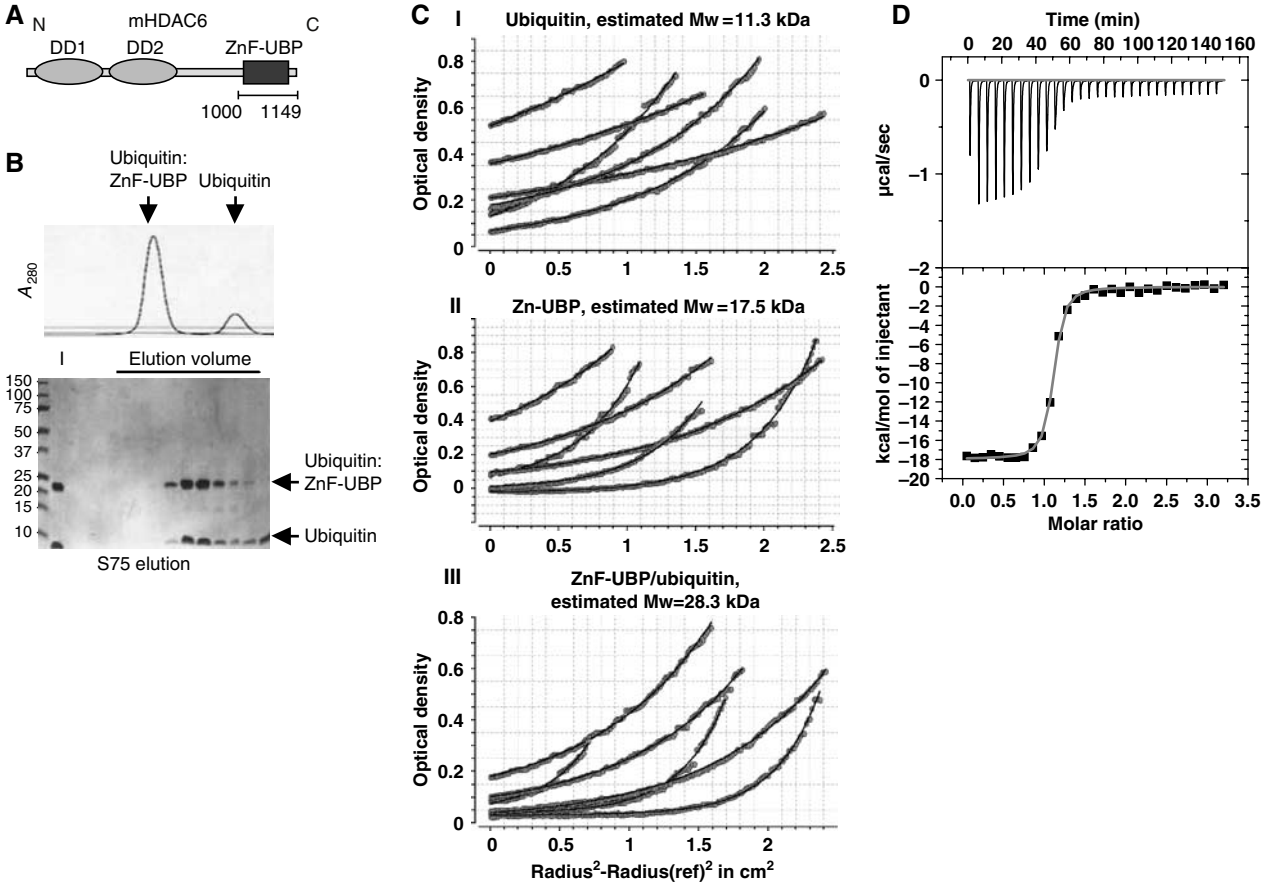

Figure 1 Characterization of the HDAC6 ZnF-UBP–ubiquitin interaction. (**A**) Schematic representation of HDAC6 functional domains. The two catalytic domains, DD1 and DD2, as well as the ubiquitin-binding domain, ZnF-UBP, of mouse HDAC6 are indicated. (**B**) HDAC6 ZnF-UBP forms a stable 1:1 complex with ubiquitin. Size-exclusion chromatography shows the formation of the HDAC6 ZnF-UBP/ubiquitin complex (upper panel). The lower panel shows the peak fractions analysed by SDS–PAGE. I stands for input. (**C**) Overlay of data (points) and fitted curves (lines) for a global analysis of equilibrium sedimentation data. The scans taken at multiple loading concentrations and multiple speeds are fit to single-component models: ubiquitin (I); HDAC6 ZnF-UBP (II); HDAC6 ZnF-UBP/ubiquitin complex (III). (**D**) ITC profile for the binding of ubiquitin to HDAC6 ZnF-UBP. Data were fitted to a one-site model. Values obtained for the binding were as follows: $K_D = 60$ nM; $\Delta H = -17.9$ kcal/mol; $-T^*\Delta S = 8.3$ kcal/mol. The stoichiometry of binding was 1:1.

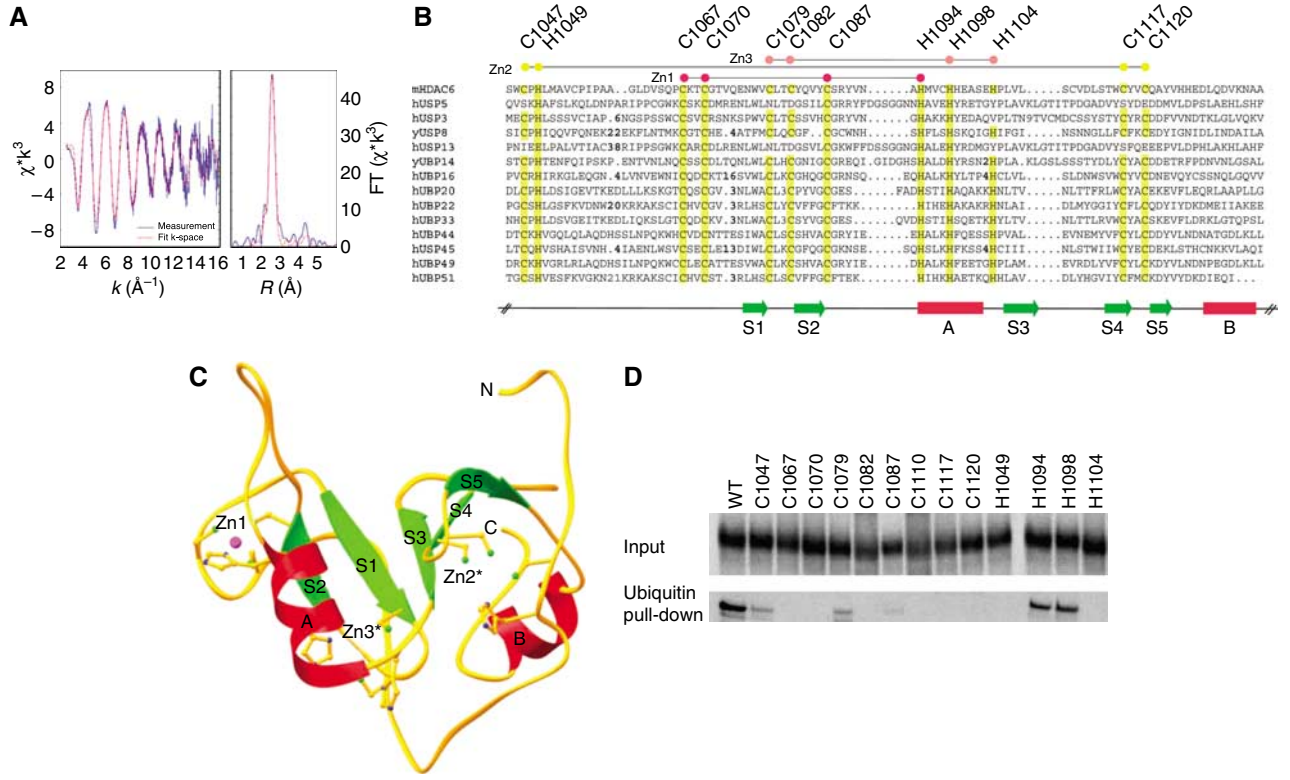

Figure 2 The HDAC6 ZnF-UBP domain contains three Zn atoms critical for ubiquitin binding. (**A**) EXAFS analysis of the HDAC6 ZnF-UBP domain was performed. Left panel: EXAFS spectrum; right panel: Fourier transformation. Experimental and theoretical spectra are represented as solid and dashed lines, respectively. The refinement resulted in an average Zn environment with 1.1 ($\pm$0.3) imidazole unit at 2.01(1) Å and 2.9 ($\pm$0.3) sulphur ligands at 2.31(1) Å. The Debye–Waller factors ($2\sigma^2 = 0.006(1)$ Å^2) and the energy shift $\Delta E_F = -9(1)$ eV with EF = 9660 eV were refined jointly for both shells. (**B**) Alignment of ZnF-UBP domains from the indicated proteins based on the crystal structure of the ZnF-UBP domain of USP5 (Reyes-Turcu *et al*, 2006). Conserved cysteine and histidine residues are highlighted. These residues cluster in positions Zn1, Zn2 and Zn3. In insertions, the number of omitted residues is marked in bold. SwissProt Database entries shown are as follows: HDAC6 (*Mus musculus*; SW: Q9Z2V5), USP5 (human; SW: P45974), UBP3 (human; SW: Q9Y6I4), UBP8 (*Saccharomyces cerevisiae*; SW: P50102), UBP13 (human; SW: Q92995), UBP14 (*S. cerevisiae*; SW: P38237), UBP16 (human; SW: Q9Y5T5), UBP20 (human; SW: Q9Y2K6), UBP22 (human; SW: Q9UPT9), UBP33 (human; SW: Q8TEY7), UBP44 (human; SW: Q9H0E7), USP45 (human; SW: Q9BRU1), UBP49 (human; SW: Q70CQ1) and UBP51 (human; SW: Q70EK9). (**C**) Ribbon representation of the USP5 ZnF-UBP domain. Zn1 corresponds to the Zn site observed in the crystal structure of USP5. Cys/His residues conserved in most ZNF-UBP domains cluster at two additional sites Zn2 and Zn3. For the ribbon diagram, USP5 residues were mutated to the corresponding Cys/His residues present in HDAC6. Asterisks indicate the predicted Zn positions. (**D**) The indicated cysteines and histidines in the ZnF-UBP domain of HDAC6 were replaced by alanine and the corresponding coding sequence (1047–1121 region of HDAC6) cloned in an expression vector. These constructs were then used to obtain ^{35}S-labelled proteins. A ubiquitin pull-down experiment was performed to evaluate the ubiquitin-binding activity of the *in vitro*-translated proteins. The input panel show 20% of the material used in the pull-down assays. Proteins retained on the ubiquitin beads are shown in the lower panel.

domain binds ubiquitin with a K_D of 3 μM (Reyes-Turcu *et al*, 2006), which roughly falls into the range of affinities for ubiquitin observed for other known ubiquitin-binding domains with K_D values ranging from 10 to 500 μM (Hicke *et al*, 2005). Interestingly, these affinities are substantially weaker than the affinity observed for the HDAC6 ZnF-UBP domain, which binds with the highest known affinity to ubiquitin.

Structural organization of the ZnF-UBP domain

In total, our construct contains 11 cysteine and 10 histidine residues. The large number of conserved cysteine and histidine residues had led to the classification of this domain as a Zn-finger-containing domain in the Conserved Domain Database (Marchler-Bauer *et al*, 2005). We used micro-focussed beam PIXE to determine the exact number of Zn atoms present in the HDAC6 ZnF-UBP domain. X-ray emission of the Zn atoms was calibrated against the relative concentration of sulphur atoms present in the HDAC6 ZnF-UBP domain (11 cysteines + 5 methionines). Several independent measurements yielded a total of 2.6 (+0.3) Zn atoms, corresponding to either two fully occupied and one partially occupied Zn-binding sites or, alternatively, to three partially occupied sites (Supplementary Table 1). We then analysed the coordination of the three Zn atoms using EXAFS (Figure 2A). EXAFS data analysis revealed an average Zn coordination by 2.9 ($\pm$0.3) cysteines and 1.1 ($\pm$0.3) histidines.

The presence of three Zn ions in the structure of the HDAC6 ZnF-UBP domain coordinated by conserved cysteine and histidine residues is supported by the crystal structure of the USP5 ZnF-UBP domain (Reyes-Turcu *et al*, 2006). Structural alignment of 14 different ZnF-UBP domains with the USP5 ZnF-UBP domain as a reference reveals conservation of eight cysteines and four histidines in most ZnF-UBP domains, but not in the USP5 ZnF-UBP domain, where eight Cys/His residues are poorly conserved (Figure 2B). Four of these 12 conserved Cys/His residues coordinate one Zn atom in a 3Cys/1His coordination (Zn1) in the USP5 ZnF-UBP

domain structure. The other eight Cys/His residues, not conserved in USP5, cluster in two regions with 3Cys/1His and 2Cys/2His coordination and tetrahedral geometry (Figure 2C). In the case of HDAC6 ZnF-UBP, the two additional Zn ions are predicted to stabilize the overall structure of the domain. In particular, Zn site 2 connects residues at the N- and C-terminal end of the domain and therefore might be particularly important for stabilization.

To further confirm the importance of the conserved Cys/His residues, we systematically mutated histidines and cysteines present in the HDAC6 ZnF-UBP domain and generally conserved in all USPs, to alanine (Figure 2B). Wild-type ZnF-UBP and its mutated versions were translated *in vitro* in a reticulocyte lysate in the presence of [^{35}S]methionine and the *in vitro*-labelled proteins were pulled down using ubiquitin-sepharose beads. Figure 2D shows that mutating all these cysteines and histidines strongly reduces efficient ubiquitin binding. However, seven cysteines and two histidines (C1067, C1070, C1082, C1087, C1110, C1117, C1120, and H1049 and H1104) were found to play an absolutely critical role in the ZnF-UBP–ubiquitin interaction. According to our structural model, all these residues (except C1110) are directly involved in Zn binding. Our results emphasize the functional importance of the Zn ions for the structural organization and stability of the HDAC6 ZnF-UBP domain as a requirement for ubiquitin binding. C1110, which does not directly coordinate Zn, corresponds to a leucine in the USP5 ZnF-UBP domain, which stabilizes the hydrophobic core. It is likely that C1110 in HDAC6 plays a similar role and mutating it into alanine would also destabilize the overall structure of the protein.

The ZnF-UBP domain controls polyubiquitin chain disassembly after induced cellular protein ubiquitination

Taking into account the extraordinary affinity of HDAC6 ZnF-UBP domain for ubiquitin, we reasoned that the HDAC6–ubiquitin complex would be unlikely to be displaced by other ubiquitin-binding proteins.

In order to test this hypothesis, we compared HDAC6 to another polyubiquitin-binding factor, RPN10, which is a polyubiquitin-binding component of the 19S proteasomal subunit.

Flag-tagged HDAC6 and RPN10 were overexpressed in Cos cells and purified (Figure 5A). Penta-ubiquitin chains (K48 5 + 1) were preincubated with equal concentrations of purified HDAC6, or purified RPN10, and then treated with the same amounts of recombinant UBPY, a ubiquitin isopeptidase (Naviglio *et al*, 1998) presenting a remarkable *in vitro* activity (Hartmann-Petersen *et al*, 2003). Figure 3 shows that HDAC6 efficiently hindered the action of UBPY and polyubiquitin chain degradation, whereas RPN10 only partially delayed the action of the protease. This experiment strongly suggests that the high-affinity ubiquitin binding by HDAC6 has the potential to stabilize the pool of cellular ubiquitinated proteins.

Accordingly, we then tested the action of HDAC6 on polyubiquitin chain turnover *in vivo*. For this purpose, 3T3 cell lines were established from HDAC6$^{-/-}$ (Zhang *et al*,

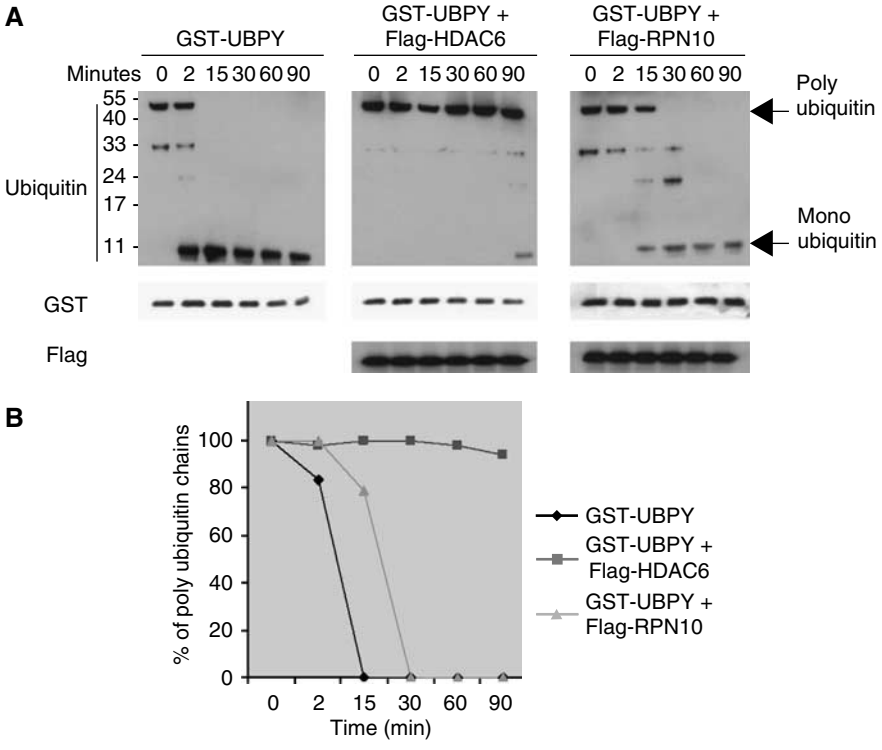

Figure 3 HDAC6 polyubiquitin masking effect. A 1 μM portion of purified penta-ubiquitin chains was pre-incubated with 6 μM of purified HDAC6 or 6 μM of purified RPN10 (see also Figure 5A). (**A**) Equivalent amounts of purified UBPY were then added and the reactions stopped at the indicated times, and the ubiquitin cleavage was visualized using an anti-ubiquitin antibody (ubiquitin panel). Anti-GST and anti-Flag antibodies were used to show the amounts of GST-UBPY and Flag-tagged proteins in each condition (indicated). (**B**) Depolymerization of polyubiquitin chain into ubiquitin monomers was monitored by Western blot and quantified and shown. 100% represents the amount of polyubiquitin at time 0.

2003; Zhang and Matthias, in preparation) or from parental HDAC6$^{+/+}$ mice. The HDAC6$^{-/-}$ cell line was also used to generate two derivatives stably re-expressing either wild-type HDAC6 or an HDAC6 mutant with an inactive ZnF-UBP domain (H1094 and H1098 changed to A). This particular HDAC6 mutant was previously shown to have completely lost its ubiquitin-binding activity (Seigneurin-Berny *et al*, 2001; Bertos *et al*, 2004). Figure 4A shows that these cells express equivalent amounts of wild-type and mutant HDAC6 at a level comparable to that of the HDAC6$^{+/+}$ 3T3 cell line (Figure 4A). As expected, the knockout of HDAC6 led to an accumulation of acetylated tubulin (Figure 4A, lane KO) and, interestingly, the re-expression of wild-type HDAC6, as well as the non ubiquitin-binding mutant of the protein (ZnF^{m}), downregulated tubulin acetylation, showing that inactivation of the ZnF-UBP domain has no effect on HDAC6 tubulin-deacetylase activity (Figure 4A, lane ZnF^{m}).

The accumulation of heavily ubiquitinated cellular proteins was induced by cell treatment with the proteasome inhibitor MG132. Cells were washed (0 h) and incubated in MG132-free medium for the indicated periods of time. Figure 4B and C shows that, compared to the HDAC6$^{+/+}$ cells, the absence of HDAC6 led to an accelerated disappearance of polyubiquitin chains. The re-expression of wild-type HDAC6 in the KO cells delayed the polyubiquitin chain decay and restored the parental cell line situation (Figure 4B and C). Remarkably, when HDAC6$^{-/-}$ cells expressed an inactive ZnF-UBP HDAC6 mutant, polyubiquitin chains rapidly disappeared, even faster than in the HDAC6$^{-/-}$ cells (Figure 4B and C). This could be owing to a dominant negative activity of this mutant titrating out other factors involved in the protection of polyubiquitin chains.

These blots were also probed with an antibody recognizing a major histocompatibility complex (MHC) class I heavy chain whose folding and assembly is subjected to quality control mechanisms leading to the degradation of defective proteins via the proteasome–ubiquitin system (Farmery and Bulleid, 2001). Figure 4B shows that MHC heavy chains, undetectable in control cells, accumulated after MG132 treatment and their degradation paralleled that of polyubiquitin chains upon MG132 removal and was dependent on HDAC6. The use of this specific proteasome substrate further confirmed our conclusions on the role of HDAC6 as a negative regulator of polyubiquitin chain turnover.

Altogether, these results show that HDAC6, through its ubiquitin-binding activity, controls the stability of the cellular pool of ubiquitinated proteins.

The chaperone-like enzyme AAA-ATPase p97/VCP is a modulator of HDAC6 ubiquitin-dependent functions

We reasoned that, owing to the high-affinity binding of HDAC6 to ubiquitin, specific cellular factors/chaperones could be required to mediate the release of HDAC6 from ubiquitin and regulate ubiquitin-dependent functions of HDAC6. The chaperone p97/VCP appeared as a very good candidate for several reasons: it interacts with HDAC6 (Seigneurin-Berny *et al*, 2001), it possesses a segregase activity, it is a positive regulator of ubiquitin/proteasome-dependent protein degradation and it negatively regulates excessive polyubiquitin chain assembly (Braun *et al*, 2002; Wang *et al*, 2003; Richly *et al*, 2005).

In order to test this hypothesis, Flag-tagged HDAC6, p97/VCP and RPN10 were expressed in Cos cells and purified as described above (Figure 5A). His-tagged penta-ubiquitin

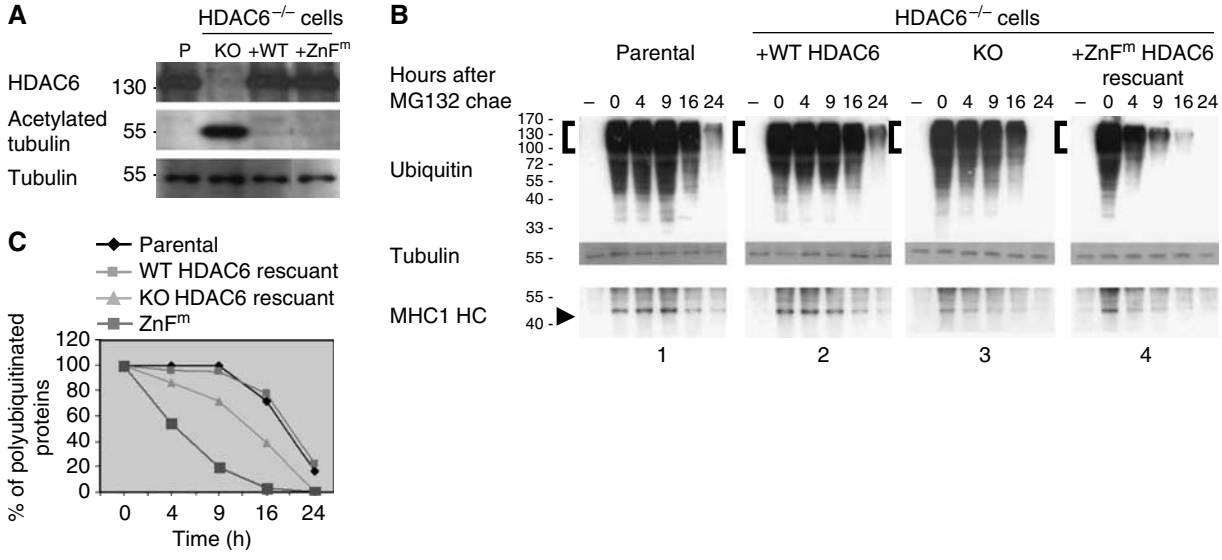

Figure 4 HDAC6 controls the turnover of polyubiquitin chains. (**A**) 3T3 cells were derived from parental HDAC6$^{+/+}$ or HDAC6$^{-/-}$ mice (KO cells). KO cells were used to establish cell lines expressing either wild-type HDAC6 (WT) or a non-ubiquitin-binding mutant of HDAC6 (ZnF^{m}). Extracts from these cells were used to monitor HDAC6 expression (HDAC6 panel). The amounts of acetylated tubulin and tubulin in the extracts were also visualized by appropriate antibodies (AcTubulin and Tubulin panels, respectively). (**B**) The accumulation of heavily ubiquitinated proteins was induced after treating cells described in panel A by the proteasome inhibitor MG132 (10 μM) for 16 h. At time $t = 0$, cells were washed and cultured in a fresh drug-free medium for the indicated times. Extracts were prepared, and ubiquitinated proteins were visualized by an anti-ubiquitin antibody. An antibody raised against an MHC class I heavy chain was also used to monitor its abundance in the same experiments (MHC HC panel). (**C**) The intensity of signals from ubiquitinated proteins in the indicated regions (brackets) was measured using the densitometric signals from the Western blots (right panel) and the values were normalized with respect to that of tubulin and plotted as a % of time 0.

chains (K48 5+1) were immobilized on Ni beads and first preincubated with an excess molar ratio of purified HDAC6. After the removal of unbound HDAC6, the beads were incubated with equal amounts of purified RPN10, p97/VCP or both (Figure 5B, input panel). The incubations were carried out in the presence or absence of ATP (Figure 5B, indicated). Following the pull-down of the beads, interactions between different proteins were detected by Western blotting. This experiments confirmed that the three studied components, HDAC6, p97/VCP and RPN10, are individually capable of polyubiquitin chain binding (lanes 2, 3 and 4). In the absence or presence of ATP, RPN10 binding was dominant over that of p97/VCP (lanes 6 and 11) and preincubation with HDAC6 prevented the binding of RNP10 to polyubiquitin (lanes 7 and 12). In the absence of ATP, ubiquitin-bound HDAC6 could also retain p97/VCP but did not allow the interaction of RNP10 with ubiquitin (compare lanes 5–8). Interestingly, in the presence of ATP, p97/VCP displaced HDAC6 and remained associated with polyubiquitin (lane 10). The addition of RNP10 to this mixture allowed the release of p97/VCP (lane 13), which formed a complex with HDAC6 in solution (Figure 5C).

These experiments suggest a mechanism through which cells may regulate the inhibitory effect of HDAC6 on polyubiquitin chain turnover. p97/VCP allows the removal of HDAC6 from polyubiquitin chains and can itself be removed by RPN10. By releasing p97/VCP from polyubiquitin chains, RPN10 actually allows the capture of p97/VCP by free HDAC6 (Figure 5C), and this could allow the recognition of ubiquitinated protein substrates by polyubiquitin-binding proteins such as RPN10.

A finely tuned balance of HDAC6 and p97/VCP concentrations determines the fate of ubiquitinated misfolded proteins

According to our data, a molar excess of HDAC6 or a decrease in p97/VCP concentration should favour protein polyubiquitination. CFTR-ΔF508, a mutant form of CFTR, which is prone to misfolding and ubiquitination, provides an appropriate model to monitor misfolded proteins aggregation (Johnston *et al*, 1998). To better visualize high molecular weight ubiquitinated forms of the protein, a truncated form of CFTR-ΔF508 (CFTR3M) was generated and its ubiquitination monitored after 6 histidine-tagged ubiquitin coexpression and capture of ubiquitinated proteins on Ni beads. Figure 6 shows that the expression of HDAC6 significantly increases the accumulation of high molecular weight CFTR3M derivatives (lane 5). Interestingly, the downregulation of p97/VCP using specific siRNA led to the same observation (lane 4). An additive effect was observed in cells treated with p97/VCP siRNA and overexpressing HDAC6 (lane 6). Ni capture approach showed that these high molecular weight CFTR3M-related proteins are indeed ubiquitinated forms. In

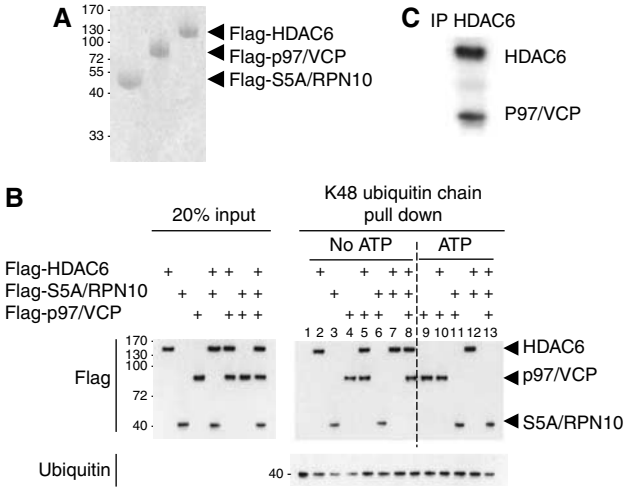

Figure 5 HDAC6–ubiquitin interaction hinders ubiquitin recognition by the ubiquitin-binding 19S protein, RPN10, and p97/VCP reverts the effect of HDAC6. (**A**) Cos cells were massively transfected with expression vectors encoding Flag-tagged HDAC6, p97/VCP and RPN10. Flag-tagged proteins were immunoprecipitated and eluted using an excess of Flag peptides and then concentrated. (**B**) His-tagged K48 5+1 ubiquitin chains were immobilized on Ni beads and incubated with an excess of purified HDAC6, RPN10 and p97/VCP. In each experiment involving HDAC6, an excess of HDAC6 was preincubated with the ubiquitin chains and, after removal of the unbound proteins, the beads were incubated with purified p97/VCP and/or RPN10 (indicated by +). After washing the beads, the proteins retained on ubiquitin were denatured and detected by the anti-Flag antibody. The experiments were performed in parallel in the absence and presence of ATP (indicated). The left panel shows the input materials. (**C**) The supernatant corresponding to the experiment shown in lane 13 was used to immunoprecipitate HDAC6 (using an anti-HDAC6 antibody) and the immunoprecipitated proteins were analysed by probing the blot with an anti-Flag antibody.

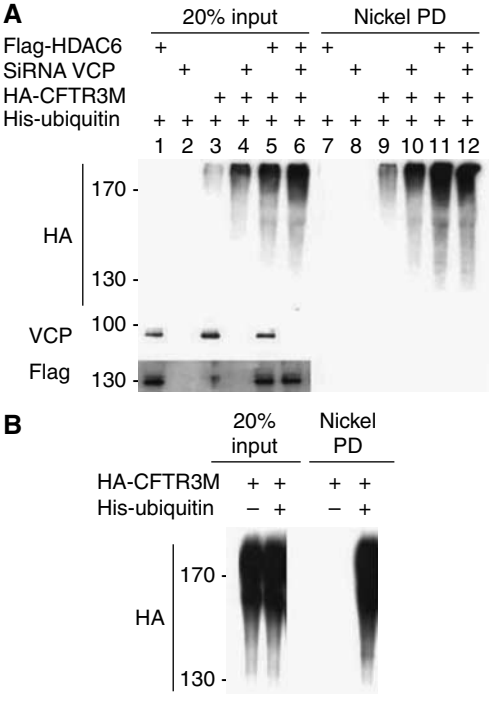

Figure 6 HDAC6–p97/VCP controlled protein polyubiquitination. (**A**) Cos cells were transfected with control siRNA or p97/VCP-specific siRNA and also with the indicated expression vectors. At 48 h post-transfection, the cells were lysed. A fraction of the lysate was kept aside (input panel) and the rest was used to capture ubiquitinated proteins on Ni beads. Input and captured materials were analysed by an anti-HA antibody. p97/VCP and Flag-HDAC6 were revealed in the input materials, and are shown at the bottom of the input panel. (**B**) CFTR3M was expressed with and without 6 His-ubiquitin (+ and −, respectively), and input and captured materials are shown.

the absence of 6 histidine-tagged ubiquitin expression, no CFTR3M could be captured by Ni beads (Figure 6B).

It had previously been shown that, owing to its ubiquitin-binding activity and its interaction with dynein motors, HDAC6 transports misfolded and ubiquitinated CFTR aggregates to aggresomes (Kawaguchi *et al*, 2003). We reasoned that by interfering with HDAC6–ubiquitin binding activity, p97/VCP should also decrease the efficiency of HDAC6 in inducing CFTR aggresome formation.

In order to test this hypothesis, HA-CFTR3M was expressed in cells alone or together with p97/VCP and the % of CFTR3M-expressing cells presenting aggresomes was determined. Ubiquitin and vimentin, known markers of aggresomes (Kawaguchi *et al*, 2003), were also detected to better identify these structures (Figure 7A). As previously reported (Kawaguchi *et al*, 2003), the expression of HDAC6 led to a marked increase in the proportion of cells forming aggresomes and the coexpression of p97/VCP significantly decreased the efficiency of aggresome formation (Figure 7B). In our hands, the treatment of cells with p97/VCP siRNA also increased the efficiency of CFTR aggresome formation (not shown). The effect of p97/VCP downregulation on aggresome formation should however be considered with caution, as, at least in yeast, Cdc48 (p97/VCP homologue) is required for normal microtubule organization (Moir *et al*, 1982) and p97/VCP downregulation may indirectly affect aggresome formation through its action on microtubules.

Altogether, our data strongly suggest that the steady-state pool of cellular polyubiquitin chains depends on a finely tuned equilibrium between the concentration of HDAC6 and p97/VCP. An imbalance of HDAC6–p97/VCP molar ratio in favour of HDAC6 would enhance the formation of ubiquitinated protein aggregates and ultimately aggresome formation.

Discussion

Using a range of biophysical approaches, we have characterized the ubiquitin-binding domain ZnF-UBP of HDAC6. MicroPIXE and EXAFS data combined with our mutational and binding analysis strongly suggest that three Zn ions organize the overall structure of the HDAC6 ZnF-UBP domain and are therefore critical for the interaction of HDAC6 ZnF-UBP with one ubiquitin molecule. Among the 10 ubiquitin-binding domains identified so far, only two ubiquitin-binding domains, the Np14 zinc-finger (NZF) and a ZnF-UBP from USP5/IsoT, also contain a Zn-binding module. However, both NZF and USP5/IsoT ZnF-UBP only contain one Zn atom ligated by four cysteine residues in the case of NZF (Alam *et al*, 2004) and by three cysteines and one histidine in the case of USP5 ZnF-UBP (Reyes-Turcu *et al*, 2006).

The particular structural organization of the HDAC6 ZnF-UBP stabilized by three Zn ions might explain the fact that it presents the highest affinity for ubiquitin among the known ubiquitin-binding domains (Hicke *et al*, 2005; Reyes-Turcu *et al*, 2006). For most ubiquitin-interacting factors, a low-affinity ubiquitin binding probably has important functional implications, as the complexes are able to rapidly undergo assembly and disassembly. Our data suggest that the HDAC6–ubiquitin interaction falls into a new functional category. In fact, the high affinity of ubiquitin binding by HDAC6 raises the issue of the regulation of the HDAC6–ubiquitin complex

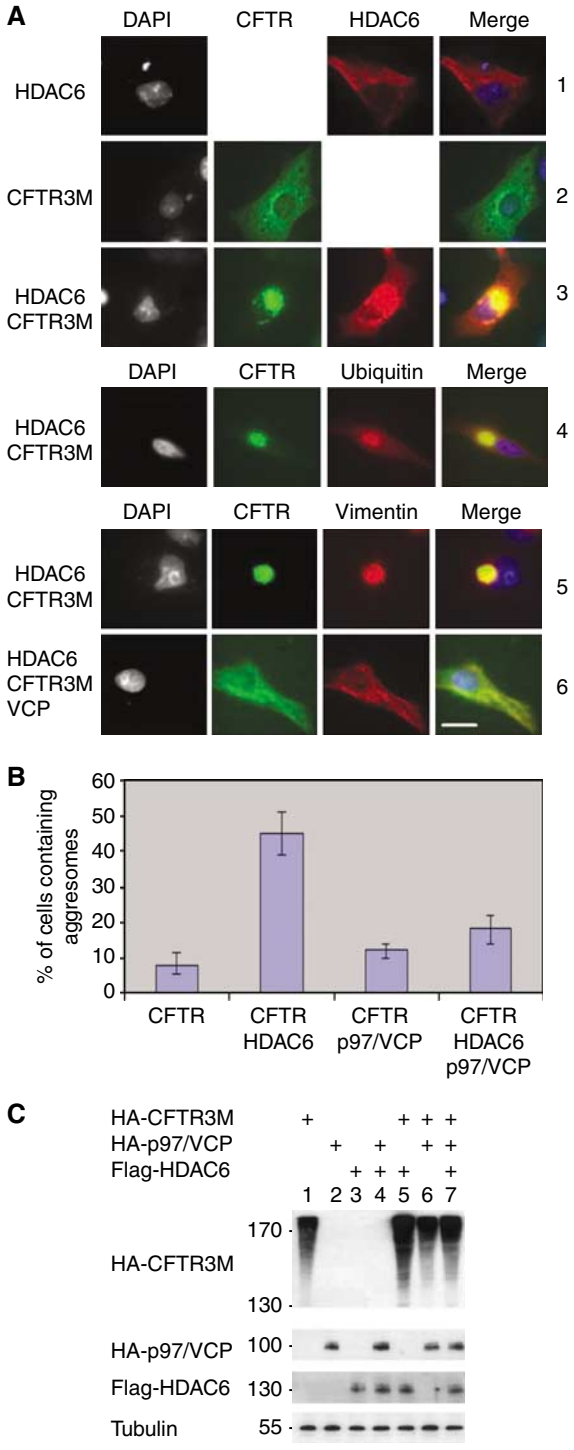

Figure 7 p97/VCP expression reduces the efficiency of HDAC6-dependent aggresome formation. (**A**) Cos cells were transfected with vectors expressing CFTR3M alone or together with HDAC6, p97/VCP or both. Cells were fixed 24 h post-transfection and different proteins were visualized. The upper panel shows the detection of HDAC6 (1), CFTR3M (2) or both (3). In the latter case, different combinations of immunodetection were used. CFTR3M was co-detected with HDAC6 (3), ubiquitin (4) or vimentin (5). The lower panels (5 and 6) show the cellular distribution of CFTR3M and vimentin in HDAC6-expressing cells, in the absence (5) or presence (6) of p97/VCP expression. (**B**) The % of cells forming CFTR3M aggresomes in each condition was determined as judged by cells containing vimentin cages and represented as a histogram. (**C**) Extracts were prepared from cells transfected in the same experiments as described above and CFTR3M, HDAC6 and p97/VCP were visualized (indicated).

dissociation. In particular, we show here that the HDAC6–polyubiquitin interaction possesses a 'masking function', preventing the action of other ubiquitin-binding factors such as USPs and ubiquitin-binding proteasomal subunits. The functional consequence of this activity of HDAC6 is a reduction of polyubiquitin turnover. It should therefore be of pivotal importance for a cell to be able to reverse this particular activity of HDAC6, in order to process polyubiquitinated proteins.

The p97/VCP chaperone was considered as an excellent candidate regulatory factor, because (i) it had previously been identified as a partner of HDAC6 (Seigneurin-Berny *et al*, 2001), and (ii) it is a chaperone involved in the control of a variety of cellular functions, many of them relying on its 'segregase' activity disassembling various complexes, including those containing ubiquitinated proteins (Wang *et al*, 2003; Romisch, 2005).

Recently, a detailed study in yeast suggested a molecular model for p97/VCP activity in the ubiquitin–proteasome protein degradation pathway. p97/VCP is proposed to restrict the ubiquitin chain elongation of a substrate protein mediated by a yeast E4, Ufd2p (Richly *et al*, 2005). Another study suggested that p97/VCP could also be involved in the control of the activity of the mammalian Ufd2p orthologue, E4B, which mediates ataxin-3 polyubiquitination. p97/VCP is thought to dissociate E4B from the polyubiquitinated ataxin-3.

Here we identify another aspect of p97/VCP function, which would also restrict an excessive accumulation of polyubiquitinated protein aggregates. Indeed, p97/VCP by dissociating HDAC6–polyubiquitin complexes favours either the action of USPs or the binding of RPN10 to the polyubiquitin chain. This suggests a novel mechanism for p97/VCP in preventing the formation of cellular inclusion bodies and acceleration of protein degradation by the proteasome.

The work of Kawaguchi *et al* (2003) shows that HDAC6 is capable of transporting ubiquitinated aggregates to the aggresome compartment. We were able to confirm these findings by showing a positive role of HDAC6 in aggresome formation. We additionally showed that this occurs under an excess of HDAC6 with respect to p97/VCP. Indeed, according to the data presented here, p97/VCP is able to recycle HDAC6 and deliver ubiquitinated proteins to the proteasome. It is expected that, under either a pathological excess of HDAC6 or a dysfunction of p97/VCP, these aggregates accumulate as aggresomes owing to irreversible binding of HDAC6 to polyubiquitin chains and to its escort activity.

In agreement with this model, the disruption of p97/VCP activities has been shown to lead to aggregate formation in various systems (Hirabayashi *et al*, 2001; Kobayashi *et al*, 2002; Nagahama *et al*, 2003; Wojcik *et al*, 2004). More interestingly, p97/VCP mutations have been identified as causing 'inclusion body myopathy associated with Paget disease of bone and frontotemporal dementia' (Watts *et al*, 2004). HDAC6 and p97/VCP therefore appear as excellent target molecules in fighting neurodegenerative diseases such as Alzheimer's disease, Parkinson's disease, Huntington's disease, amyotrophic lateral sclerosis and prion diseases, which are increasingly recognized as having common molecular mechanisms, including protein aggregation and inclusion body formation.

Although this work emphasizes the function of HDAC6 as a factor negatively regulating proteasomal protein degradation, we believe that, under physiological concentrations of HDAC6 and p97/VCP, HDAC6 may also accelerate protein degradation. Indeed, HDAC6 by favouring protein polyubiquitination and p97/VCP by allowing the delivery of the ubiquitinated substrates should facilitate efficient protein ubiquitination and degradation.

In conclusion, we propose here that HDAC6–p97/VCP constitutes a key cellular management system, which decides the fate of ubiquitinated cellular proteins.

Materials and methods

Methods for analytical ultracentrifugation, ITC, EXAFS experiments and microPIXE analysis are accessible in Supplementary data.

HDAC6$^{-/-}$ cell line and the re-expression of HDAC6

Mice with invalidated HDAC6 gene were generated (Zhang *et al*, 2003; Zhang and Matthias, data not shown) and mouse embryo fibroblasts were isolated from E13.5 embryos. 3T3 cell lines were established following a standard 3T3 protocol. Wild-type and mutant HDAC6 cDNAs were cloned into a pMSCV.EGFP vector. The retrovirus was made from Phoenix cells following standard protocols. The HDAC6$^{-/-}$ 3T3 cells were infected and kept in culture for 2 weeks and single GFP-positive cells were sorted into 96-well plates.

Cell culture, transfection assays, siRNA treatment and in situ immunodetection procedure

Cells were maintained in DMEM supplemented with 10% fetal calf serum and seeded in appropriate plates and grown to 60–70% confluence on the day of transfection. Transfections were performed with Lipofectamine 2000 (Invitrogen), using 5 μl Lipofectamine and various quantities of expression vectors or empty vectors for a total of 5 μg DNA.

p97/VCP siRNAs were designed as previously described (Wojcik *et al*, 2004) and purchased from Eurogentec. Control siRNAs were inactive siRNAs against HAT1 (not shown). HeLa cells were seeded in six-well plates at 10^5 cells/well 24 h before siRNA treatment. *In situ* immunofluorescence analysis was carried out as described previously (Matsuyama *et al*, 2002).

Plasmids and antibodies

HDAC6 expression vectors were previously described (Verdel *et al*, 2000; Seigneurin-Berny *et al*, 2001). HA- and Flag-p97/VCP were cloned in pcDNA.3 vectors after PCR amplification of its coding sequence from a mouse embryo bank (Clonthec). GFP-CFTR-ΔF508 expression vector was kindly provided by Dr Kopito. Flag-RPN10 expression vector was a kind gift of Dr Minoru Yoshida. pSG His-ubiquitin was a gift of Dr Bohman. pGEXKG-UBPY plasmid was a kind gift of Dr Hartmann-Petersen. CFTR-ΔF508 mutant lacked its C-terminal ATPase domain (deletion of 1057–1480 region). GST-Cterminal part of HDAC6 was cloned in pGEX4-T-1 vector (Amersham) after a PCR amplification of the corresponding sequence with the following primers : 5′ccc ctt cgg cga cct cca gtc ctg tac ttg3′ and 5′gtg tga gtg ggg cat gtc ctc ccc aaa3′. p97/VCP antibody was a gift of Dr Tonks. Anti-HDAC6 was described previously (Seigneurin-Berny *et al*, 2001). Anti-MHC class I heavy chain was a monoclonal antibody against haplotype H2Dd (Cedarlane Labs, CL9009B).

Purification of HDAC6 C-terminal part and ubiquitin

GST-Cter was expressed in BL21 (DE3)pLysS strain (Stratagene), and after purification on glutathione sepharose resin (Sigma), the GST tag was removed with thrombin (Sigma) and the HDAC6 part was purified to homogeneity after phenyl sepharose column and S75 gel filtration (Amersham). The ubiquitin sequence was amplified by PCR and cloned in pETM13, as His-tagged fusion and expressed in BL21(DE3) strain (Stratagene) and purified on nickel probond resin (Invitrogen) and purified to homogeneity by S75 gel filtration (Amersham).

Site-directed mutagenesis, protein purification and ubiquitin binding assays

HDAC6 C-terminal part cloned in pET28a+ (Novagen) and mutagenized using the QuickChange site-directed PCR mutagenesis (Stratagene) and the resulting mutations were controlled after sequencing. The corresponding ^{35}S-labelled proteins were generated in a reticulocyte lysate (Promega) and pull-downs were performed as described previously (Seigneurin-Berny *et al*, 2001).

Flag-tagged HDAC6, p97/VCP and RPN10 were overexpressed in Cos7 cells after massive transfection and the tagged proteins were immunoprecipitated using M2 coupled beads and purified using a Flag-peptide elution procedure (Sigma). Proteins were eluted in ubiquitin-binding buffer and then concentrated using Centricon concentrator (Millipore).

Penta-ubiquitin binding assays were performed as follows: 1 μM of purified His-tagged penta-ubiquitin ($ubiquitin_5^{+1}$ from Affinity) was immobilized on Ni beads and preincubated with 6 μM Flag-HDAC6 for 30 min at room temperature. A 6 μM portion of Flag-p97/VCP or Flag-RPN10 or both was then added. Binding reactions were performed in 50 mM Tris pH 7.4, 150 mM NaCl, 1 mM β-mercaptoethanol, 2% of glycerol, anti-protease inhibitor (Roche) with or without 200 μM ATP and 200 μM $MgCl_2$, during 30 min at room temperature.

Unbound proteins were removed by centrifugation. Proteins retained were eluted by electrophoresis sample buffer. Unbound HDAC6–p97/VCP complex, after the ATP-dependent action of p97/VCP, was immunoprecipitated using an anti-HDAC6 antibody (Seigneurin-Berny *et al*, 2001) and the proteins detected by Western.

Polyubiquitin chain depolymerization assays

A 1 μM portion of ubiquitin chains in ubiquitin-binding buffer was preincubated at 37°C with 6 μM of purified Flag-HDAC6 or 6 μM of purified Flag-RPN10. GST-UBPY (6 μM) was then added for different times. Reactions were blocked by SDS–PAGE loading buffer, and ubiquitin, GST and Flag-tagged proteins were detected.

Supplementary data

Supplementary data are available at *The EMBO Journal* Online.

Acknowledgements

We gratefully acknowledge the association 'vaincre la mucoviscidose' for supporting CB with PhD fellowship for 4 years. BG was supported by 'association pour la recherche sur le cancer' for his fourth year of PhD fellowship. SK laboratory was supported by 'region Rhône Alpes theme prioritaire Cancer' programme and CLARA cancéropôle. We gratefully acknowledge the expert assistance of Sandrine Benitski in tissue culture work. The work in PM laboratory was supported by the Novartis Research Foundation. We thank the Ion Beam Centre at the University of Surrey, Guildord, UK for facilities access and Dr I Gomez-Morilla for beamline assistance there.

References

Alam SL, Sun J, Payne M, Welch BD, Blake BK, Davis DR, Meyer HH, Emr SD, Sundquist WI (2004) Ubiquitin interactions of NZF zinc fingers. *EMBO J* **23:** 1411–1421

Amerik AY, Li SJ, Hochstrasser M (2000) Analysis of the deubiquitinating enzymes of the yeast *Saccharomyces cerevisiae*. *Biol Chem* **381:** 981–992

Bertos NR, Gilquin B, Chan GK, Yen TJ, Khochbin S, Yang XJ (2004) Role of the tetradecapeptide repeat domain of human histone deacetylase 6 in cytoplasmic retention. *J Biol Chem* **279:** 48246–48254

Braun S, Matuschewski K, Rape M, Thoms S, Jentsch S (2002) Role of the ubiquitin-selective CDC48(UFD1/NPL4)chaperone (segregase) in ERAD of OLE1 and other substrates. *EMBO J* **21:** 615–621

Destaing O, Saltel F, Gilquin B, Chabadel A, Khochbin S, Ory S, Jurdic P (2005) A novel Rho–mDia2–HDAC6 pathway controls podosome patterning through microtubule acetylation in osteoclasts. *J Cell Sci* **118:** 2901–2911

Farmery MR, Bulleid NJ (2001) Major histocompatibility class I folding, assembly, and degradation: a paradigm for two-stage quality control in the endoplasmic reticulum. *Prog Nucleic Acid Res Mol Biol* **67:** 235–268

Ghislain M, Dohmen RJ, Levy F, Varshavsky A (1996) Cdc48p interacts with Ufd3p, a WD repeat protein required for ubiquitin-mediated proteolysis in *Saccharomyces cerevisiae*. *EMBO J* **15:** 4884–4899

Grozinger CM, Hassig CA, Schreiber SL (1999) Three proteins define a class of human histone deacetylases related to yeast Hda1p. *Proc Natl Acad Sci USA* **96:** 4868–4873

Hartmann-Petersen R, Hendil KB, Gordon C (2003) Ubiquitin binding proteins protect ubiquitin conjugates from disassembly. *FEBS Lett* **535:** 77–81

Hicke L, Schubert HL, Hill CP (2005) Ubiquitin-binding domains. *Nat Rev Mol Cell Biol* **6:** 610–621

Hirabayashi M, Inoue K, Tanaka K, Nakadate K, Ohsawa Y, Kamei Y, Popiel AH, Sinohara A, Iwamatsu A, Kimura Y, Uchiyama Y, Hori S, Kakizuka A (2001) VCP/p97 in abnormal protein aggregates, cytoplasmic vacuoles, and cell death, phenotypes relevant to neurodegeneration. *Cell Death Differ* **8:** 977–984

Hook SS, Orian A, Cowley SM, Eisenman RN (2002) Histone deacetylase 6 binds polyubiquitin through its zinc finger (PAZ domain) and copurifies with deubiquitinating enzymes. *Proc Natl Acad Sci USA* **99:** 13425–13430

Hubbert C, Guardiola A, Shao R, Kawaguchi Y, Ito A, Nixon A, Yoshida M, Wang XF, Yao TP (2002) HDAC6 is a microtubule-associated deacetylase. *Nature* **417:** 455–458

Johnson ES, Ma PC, Ota IM, Varshavsky A (1995) A proteolytic pathway that recognizes ubiquitin as a degradation signal. *J Biol Chem* **270:** 17442–17456

Johnston JA, Ward CL, Kopito RR (1998) Aggresomes: a cellular response to misfolded proteins. *J Cell Biol* **143:** 1883–1898

Kawaguchi Y, Kovacs JJ, McLaurin A, Vance JM, Ito A, Yao TP (2003) The deacetylase HDAC6 regulates aggresome formation and cell viability in response to misfolded protein stress. *Cell* **115:** 727–738

Kobayashi T, Tanaka K, Inoue K, Kakizuka A (2002) Functional ATPase activity of p97/valosin-containing protein (VCP) is required for the quality control of endoplasmic reticulum in neuronally differentiated mammalian PC12 cells. *J Biol Chem* **277:** 47358–47365

Kovacs JJ, Murphy PJ, Gaillard S, Zhao X, Wu JT, Nicchitta CV, Yoshida M, Toft DO, Pratt WB, Yao TP (2005) HDAC6 regulates Hsp90 acetylation and chaperone-dependent activation of glucocorticoid receptor. *Mol Cell* **18:** 601–607

Marchler-Bauer A, Anderson JB, Cherukuri PF, DeWeese-Scott C, Geer LY, Gwadz M, He S, Hurwitz DI, Jackson JD, Ke Z, Lanczycki CJ, Liebert CA, Liu C, Lu F, Marchler GH, Mullokandov M, Shoemaker BA, Simonyan V, Song JS, Thiessen PA, Yamashita RA, Yin JJ, Zhang D, Bryant SH (2005) CDD: a conserved domain database for protein classification. *Nucleic Acids Res* **33:** D192–D196

Matsuyama A, Shimazu T, Sumida Y, Saito A, Yoshimatsu Y, Seigneurin-Berny D, Osada H, Komatsu Y, Nishino N, Khochbin S, Horinouchi S, Yoshida M (2002) *In vivo* destabilization of dynamic microtubules by HDAC6-mediated deacetylation. *EMBO J* **21:** 6820–6831

Moir D, Stewart SE, Osmond BC, Botstein D (1982) Cold-sensitive cell-division-cycle mutants of yeast: isolation, properties, and pseudoreversion studies. *Genetics* **100:** 547–563

Mullally JE, Chernova T, Wilkinson KD (2006) Doa1 is a Cdc48 adapter that possesses a novel ubiquitin binding domain. *Mol Cell Biol* **26:** 822–830

Nagahama M, Suzuki M, Hamada Y, Hatsuzawa K, Tani K, Yamamoto A, Tagaya M (2003) SVIP is a novel VCP/p97-interacting protein whose expression causes cell vacuolation. *Mol Biol Cell* **14:** 262–273

Naviglio S, Mattecucci C, Matoskova B, Nagase T, Nomura N, Di Fiore PP, Draetta GF (1998) UBPY: a growth-regulated human ubiquitin isopeptidase. *EMBO J* **17:** 3241–3250

Reyes-Turcu FE, Horton JR, Mullally JE, Heroux A, Cheng X, Wilkinson KD (2006) The ubiquitin binding domain ZnF UBP

recognizes the C-terminal diglycine motif of unanchored ubiquitin. *Cell* **124:** 1197–1208

Richly H, Rape M, Braun S, Rumpf S, Hoege C, Jentsch S (2005) A series of ubiquitin binding factors connects CDC48/p97 to substrate multiubiquitylation and proteasomal targeting. *Cell* **120:** 73–84

Rumpf S, Jentsch S (2006) Functional division of substrate processing cofactors of the ubiquitin-selective Cdc48 chaperone. *Mol Cell* **21:** 261–269

Romisch K (2005) Endoplasmic reticulum-associated degradation. *Annu Rev Cell Dev Biol* **21:** 435–456

Seigneurin-Berny D, Verdel A, Curtet S, Lemercier C, Garin J, Rousseaux S, Khochbin S (2001) Identification of components of the murine histone deacetylase 6 complex: link between acetylation and ubiquitination signaling pathways. *Mol Cell Biol* **21:** 8035–8044

Verdel A, Curtet S, Brocard MP, Rousseaux S, Lemercier C, Yoshida M, Khochbin S (1999) Identification of a new family of higher eukaryotic histone deacetylases. Coordinate expression of differentiation-dependent chromatin modifiers. *J Biol Chem* **274:** 2440–2445

Verdel A, Curtet S, Brocard MP, Rousseaux S, Lemercier C, Yoshida M, Khochbin S (2000) Active maintenance of mHDA2/mHDAC6 histone-deacetylase in the cytoplasm. *Curr Biol* **10:** 747–749

Wang B, Alam SL, Meyer HH, Payne M, Stemmler TL, Davis DR, Sundquist WI (2003) Structure and ubiquitin interactions of the conserved zinc finger domain of Npl4. *J Biol Chem* **278:** 20225–20234

Watts GD, Wymer J, Kovach MJ, Mehta SG, Mumm S, Darvish D, Pestronk A, Whyte MP, Kimonis VE (2004) Inclusion body myopathy associated with Paget disease of bone and frontotemporal dementia is caused by mutant valosin-containing protein. *Nat Genet* **36:** 377–381

Wojcik C, Yano M, DeMartino GN (2004) RNA interference of valosin-containing protein (VCP/p97) reveals multiple cellular roles linked to ubiquitin/proteasome-dependent proteolysis. *J Cell Sci* **117:** 281–292

Zhang Y, Li N, Caron C, Matthias G, Hess D, Khochbin S, Matthias P (2003) HDAC-6 interacts with and deacetylates tubulin and microtubules *in vivo*. *EMBO J* **22:** 1168–1179